

# A Novel Three-Dimensional Glioma Blood Brain Barrier Model for High Throughput Testing of Tumorcidal Capability

CORNING

## Application Note

Hilary Sherman and Ann Rossi, Ph.D.  
Corning Incorporated, Life Sciences  
Kennebunk, ME USA

### Introduction

The blood brain barrier (BBB) limits passage of substances between general circulation and the brain extracellular fluid, maintaining homeostasis in neural tissues and providing a defense against potential toxins. However, the protection provided by the BBB often prevents conventional chemotherapeutics from reaching brain tumors which makes brain cancers one of the most difficult cancers to treat<sup>1</sup>. Traditionally, high throughput testing of compound permeability through the BBB *in vitro* has been limited to assay of radio- or fluorophore-labeled compounds as they pass a cell monolayer growing on a permeable support system. Unfortunately, the labels themselves may negatively impact the assay, and the ability to determine resulting tumor cytotoxicity must be studied independently. Here, we demonstrate a three dimensional (3D) model to study label-free BBB transport as well as the resulting brain tumor cytotoxicity by combining two commercially available products: Corning® 96-well spheroid microplates and the HTS Transwell®-96 tissue culture system. Corning spheroid microplates are cell culture microplates with round well-bottom geometry coated with Corning Ultra-Low Attachment surface, enabling the formation of a single multi-cellular tumor spheroid centered in each well in a highly reproducible manner. HTS Transwells are permeable support systems commonly used for drug transport and migration/invasion studies. By replacing the standard flat-bottom Transwell receiver plate with a Corning spheroid microplate, we have developed a more comprehensive assay to study drug transport across the BBB and the resulting 3D glioma spheroid toxicity in an easy-to-use, 3D, high throughput assay.

### Materials and Methods

For the blood brain barrier, MDCKII/MDR1 cells were attained from Dr. Piet Borst (Netherlands Cancer Institute, Amsterdam, Netherlands) and seeded into HTS 96-well Transwells (Corning Cat. No. 3391 or 7369) at  $1 \times 10^5$  cells/cm<sup>2</sup> in 100  $\mu$ L of Dulbecco's Modification of Eagle's Medium (DMEM; Corning Cat. No. 10-013-CM) supplemented with 10% fetal bovine serum (FBS; Corning Cat. No. 35-010-CV). Cells were cultured for 5 days with a medium exchange 24 hours prior to assay. Monolayer integrity and P-glycoprotein (P-gp) pump function were assessed via lucifer yellow (LY; MilliporeSigma Cat. No. L0144) and rhodamine 123 permeability (Rh123; MilliporeSigma Cat. No. R8004), respectively. MDCKII/MDR1 monolayers were immunostained to confirm presence of tight junction proteins ZO-1 (Thermo Fisher

Cat. No. 33-918-8) and occludin (Thermo Fisher Cat. No. 33-158-8) per manufacturer's protocol. Nuclei were counterstained with 1  $\mu$ g/mL Hoechst 34580 (Thermo Fisher Cat. No. H21486).

LN-229 cells (ATCC® Cat. No. CRL-2611™) were routinely cultured in DMEM containing 10% FBS to be used for the glioblastoma model. Cells were harvested with Accutase® cell detachment solution (Corning Cat. No. 25-058-CI), seeded into the Corning 96-well spheroid microplates at  $1 \times 10^3$  cells in 50  $\mu$ L per well, and incubated for 24 hours prior to assay to form 3D spheroids. For initial drug testing, spheroids were exposed to varying concentrations of cisplatin (Thermo Fisher Cat. No. 1134357) and piperlongumine (MilliporeSigma Cat. No. 528124) by adding 50  $\mu$ L of drug or vehicle control and culturing for 48 hours. Cisplatin was reconstituted in Dulbecco's Phosphate-Buffered Saline (DPBS; Corning Cat. No. 21-031-CM) while piperlongumine was initially dissolved in DMSO. After drug exposure, 100  $\mu$ L/well of CellTiter-Glo® 3D (Promega Cat. No. G9683) was added to assess cell viability. Luminescence was detected using a PerkinElmer EnVision Multimode Plate Reader.

In order to combine BBB HTS 96-well Transwells with LN-229 spheroids, medium was removed from 5-day-old MDCKII/MDR1 monolayers and medium in the apical chamber was replaced with 250  $\mu$ M cisplatin, piperlongumine, or medium containing vehicle controls. Inserts with and without MDCKII/MDR1 cells were then combined with spheroid microplates containing 24-hour-old LN-229 spheroids in 200  $\mu$ L per well of medium for 2 hours at 37°C. A schematic of the Transwell and spheroid plate set up is shown in Diagram 1. After 2 hours of co-incubation, inserts were removed and tested for lucifer yellow permeability in order to ensure barrier integrity remained. LN-229 spheroids were cultured for 2 additional days and then assessed for viability as previously described with the following exception: medium was removed and replaced with a 200  $\mu$ L of CellTiter-Glo 3D diluted 1:1 with medium.

For the drug screen, the BBB and LN-229 spheroids were set up as previously described. After 5 days of BBB formation, medium from Transwells was aspirated and the apical chamber medium was replaced with 50  $\mu$ L of compound from the Tocriscreen™ Kinase Inhibitor Toolbox (Tocris Bioscience Cat. No. 3514) or media containing vehicle. Inserts were then combined with 24-hour-old LN-229 spheroids for 2 hours at 37°C. After 2 hours of co-incubation, inserts were removed, tested for barrier integrity, and LN-229 spheroids were cultured and assayed as described previously.

## Results and Discussion

### Blood Brain Barrier Model

Historically, MDCKII/MDR1 cells have been used to create *in vitro* models to test for BBB permeability<sup>2,3</sup>. To demonstrate the effectiveness of our MDCKII/MDR1 BBB model we assessed formation of tight junctions, monolayer integrity, and P-gp pump function. Formation of tight junctions was verified by immunofluorescence staining of the tight junction-associated proteins ZO-1 and occludin. Confocal images clearly show both positive ZO-1 and occludin staining between cells (Figure 1). The tightness of the monolayer was assessed by measuring leakage of LY from the apical compartment of the Transwell insert to the basolateral compartment over the course of 1 hour (Figure 2A). In this study, the LY permeability value was ~1 nm/sec., consistent with a continuous monolayer. Cell monolayers with LY permeability values less than 20 nm/sec. are considered intact<sup>4</sup>. Additionally, Figure 2B shows

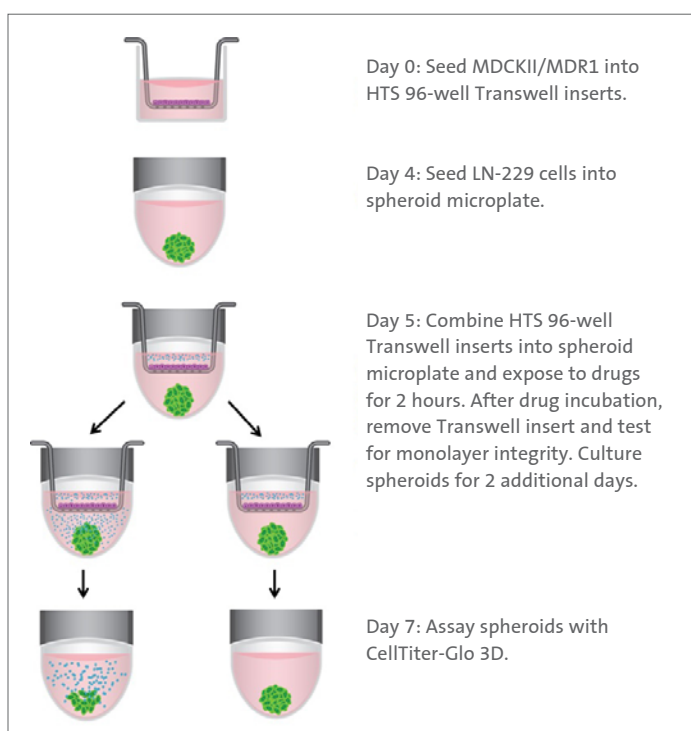


Diagram 1. Schematic of assay set up.

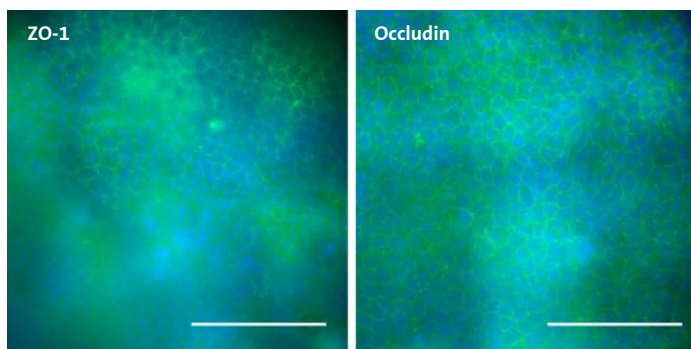


Figure 1. Presence of tight junction proteins in MDCKII/MDR1 monolayer. Representative confocal images of ZO-1(left) and occludin (right) immunofluorescence (green). Images were acquired with a 40X objective on the CX7 CellInsight. Nuclei are counterstained with Hoechst (blue). Scale bars = 100  $\mu\text{m}$ .

higher efflux of Rh123—a known substrate of the P-gp pump—in the basolateral-to-apical direction. Comparison of the basolateral-to-apical and apical-to-basolateral effluxes yields an efflux ratio  $>29$ , indicative of a functioning P-gp pump<sup>5</sup>.

### Spheroid Toxicity

To demonstrate the utility of the BBB model, the effects of two known cytotoxic drugs, cisplatin and piperlongumine were tested. A concentration-dependent response was achieved when both compounds were added directly to LN-229 spheroids at varying concentrations (Figure 3). Cisplatin is known to induce cytotoxicity to cancer cells but is incapable of penetrating the BBB at high enough levels to be effective<sup>6</sup>. Piperlongumine, on the other hand, not only has shown cancer-specific cytotoxicity but has demonstrated the capability of crossing the BBB at high levels<sup>7-9</sup>. By combining the HTS 96-well Transwells with the LN-229 spheroids we were able to recapitulate the *in vivo* behavior of the two drugs (Figure 4). Piperlongumine induced cytotoxicity regardless of the presence of a BBB. In contrast, there was a statistically significant reduction in cytotoxic effect observed with cisplatin when the BBB was present.

The BBB model was further tested with a screen of a small library of kinase inhibitors to determine if cytotoxicity of the

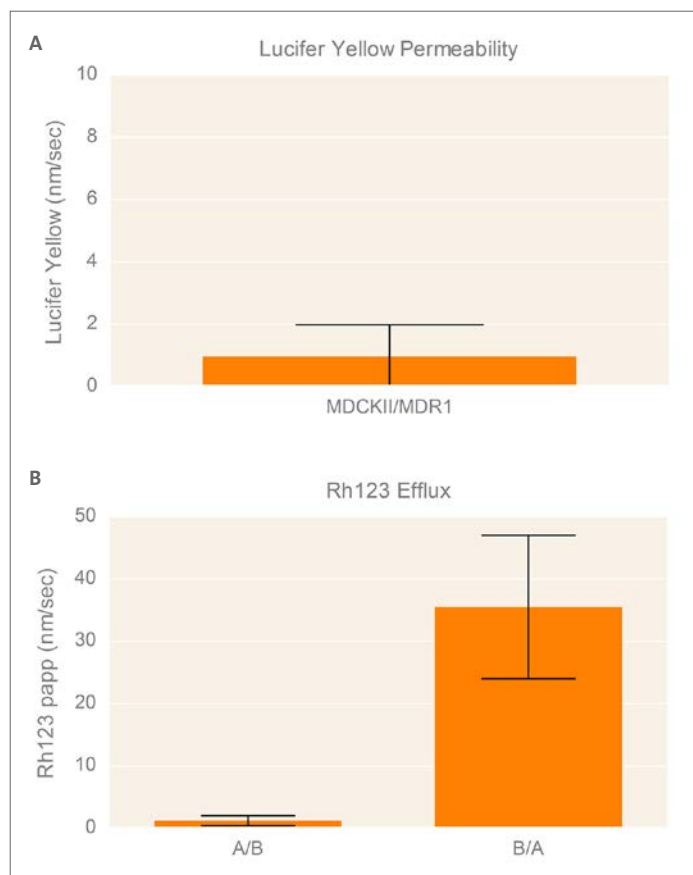
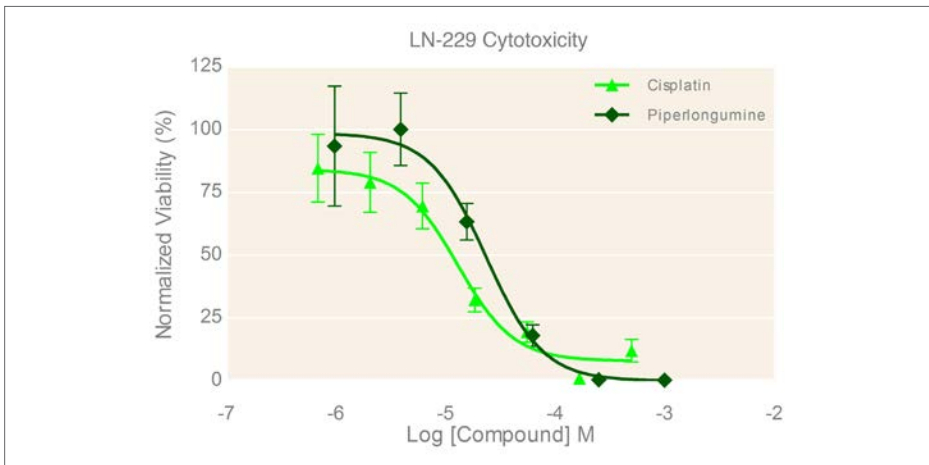


Figure 2. MDCKII/MDR1 cell monolayers form functional barriers. (A) Lucifer yellow permeability was measured at  $0.96 \pm 1.03$  nm/sec. Low lucifer yellow permeability ( $<20$  nm/sec) indicates a tight monolayer<sup>4</sup>. (B) Rh123 apparent permeability (Papp) indicated stronger efflux in the basolateral-to-apical (B/A) compared to the apical-to-basolateral direction (A/B). Efflux ratio was 29 nm/sec., indicative of functional P-gp pumps. Mean  $\pm$  SD. N = 120 for 3 independent tests.

gliomaspheres was dependent upon BBB permeability. Kinase inhibition is currently a target for several different cancer therapeutics, and the Tocris library provided a small curated group of compounds to test in this proof-of-principle study. Figure 5 shows a representative screen of the drug library and buffer controls performed with and without a BBB on the HTS 96-well Transwell® inserts. A hit was identified as a compound with a relative

luminescent (RLU) value of less than  $3\sigma$  of the buffer response. More cytotoxic hits were identified in the absence of the BBB. In 3 independent screens, only 9 of those 27 hits (Figure 5, inset) were also positive with the addition of the Transwell BBB. Importantly, co-culture of the spheroids with BBB narrowed the hit list. This subset represents true positives in the assay and potential leads for therapeutic indications.



**Figure 3. Concentration-dependent cytotoxicity of LN-229 spheroids.** LN-229 viability after 48 hours of exposure to varying concentrations of cisplatin and piperlongumine. Normalized viability was calculated by comparing luminescent signal in the presence of drug to that of buffer plus vehicle controls. Mean  $\pm$  SD. N = 12 wells per concentration from 2 independent studies.

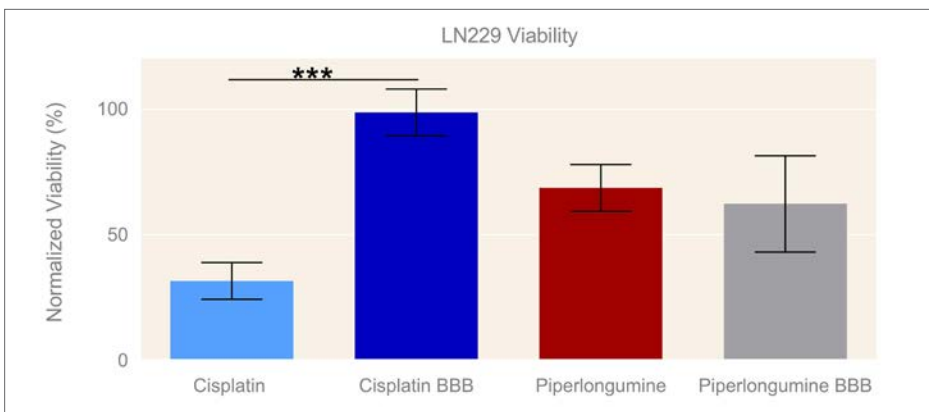


**Figure 4. Model demonstrates *in vivo*-like cytotoxic response.** LN-229 viability 48 hours after a 2-hour exposure to 250  $\mu$ M cisplatin or piperlongumine. Percent viability was calculated by comparing luminescent signal in the presence of drug to that of buffer plus vehicle controls. Two-tailed t-test indicated a statistically significant difference between cisplatin-induced cytotoxicity with and without a BBB. \*\*\* =  $p < 0.0001$ . Mean  $\pm$  SD. N = 30 from 3 independent studies.

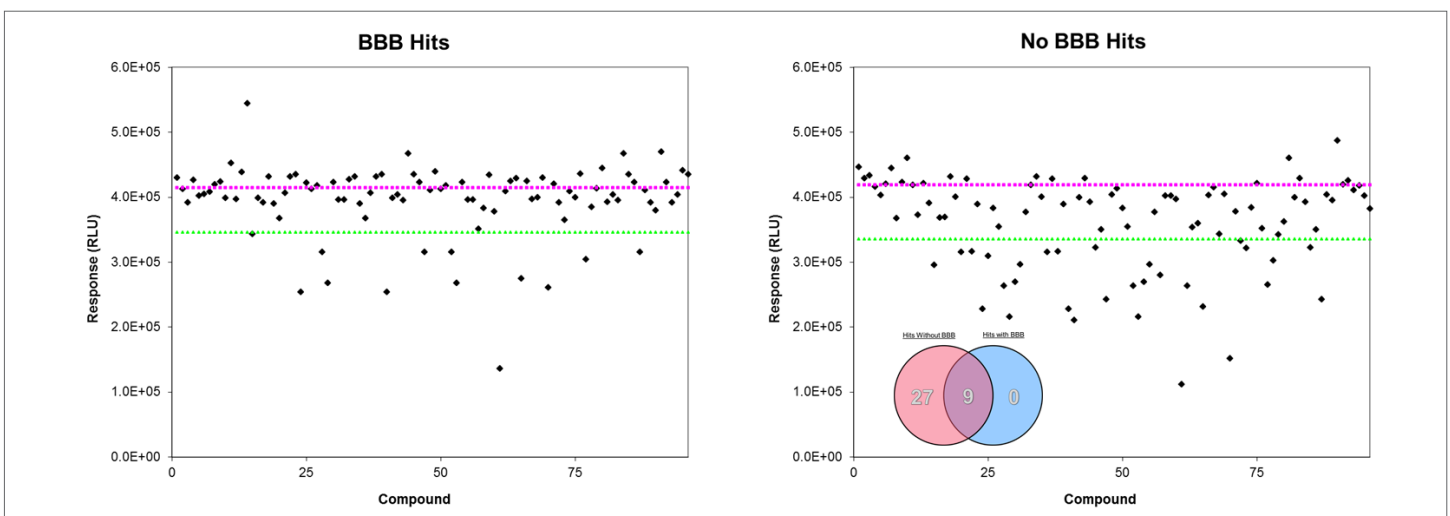


**Figure 5. BBB narrows list of cytotoxic hits in small library screen.** Representative LN-229 viability data with (left) and without (right) BBB model from screen of 80-drug library. Pink line is average buffer response and green line represents  $3\sigma$  below buffer response. Data points below green line were considered hits. Hits were considered if they were  $3\sigma$  below buffer response in at least 2 of 3 independent screens. A fraction of hits in the absence of BBB were identified in the presence of BBB from 3 screens (inset).

## Conclusions

In order to create a model system to investigate BBB transport and gliosphere cytotoxicity in a single, high throughput assay, we combined Corning® 96-well spheroid microplates and HTS 96-well Transwell® inserts. Previously, separate studies have been required to investigate gliosphere toxicity independently from BBB transport. The model presented here is intended for identification of therapeutic compounds that can both permeate the BBB and induce cytotoxicity of tumor spheroids. By extension, healthy neurospheres could be combined with the BBB in this model and employed for drug counterscreens to identify off-target effects on neural tissue. Regardless of the cell type chosen, the system described here is a more comprehensive, more *in vivo*-like model with which researchers can test the ability for a compound, cell or cell product to pass the BBB while simultaneously looking at the impact on a 3D structure.

## References

1. Bhowmik A, Khan R, Ghosh. Blood brain barrier: a challenge for effectual therapy of brain tumors. *Biomed Res Int* 2015;2015:320941. doi:10.1155/2015/320941.
2. Wang Q, Rager JD, Weinstein K, Kardos PS, Dobson GL, Li J, et al. Evaluation of the MDR-MDCK cell line as a permeability screen for the blood-brain barrier. *Int J Pharm* 2005;288(8):349-359. doi:10.1016/j.ijpharm.2004.10.007.
3. Lv H, Zhang X, Sharma J, Reddy MVR, Reddy EP, Gallo JM. Integrated pharmacokinetic-driven approach to screen candidate anticancer drugs for brain tumor chemotherapy. *AAPS J* 2013;15(1):250-257. doi:10.1208/s12248-012-9428-4.
4. Rautio J, Humphreys JE, Webster LO, Balakrishnan A, Keogh JP, Kunta JR, et al. In vitro p-glycoprotein inhibition assays for assessment of clinical drug interaction potential of new drug candidates: a recommendation for probe substrates. *Drug Metab Dispos* 2006;34(5):786-792. doi:10.1124/dmd.105.008615.
5. U.S. Food and Drug Administration/Center for Drug Evaluation and Research. In vitro metabolism-and transporter-mediated drug-drug interaction studies guidance for industry. Silver Spring, MD. 2017.
6. Stewart DJ, Leavens M, Maor M, Feun L, Luna M, Bonura J, et al. Human central nervous system distribution of cis-diamminedichloroplatinum and use as a radiosensitizer in malignant brain tumors. *Cancer Res* 1982;42(6):2474-2479.
7. Raj L, Ide T, Gurkar AU, Foley M, Schenone M, Li X, et al. Selective killing of cancer cells by a small molecule targeting the stress response to ROS. *Nature* 2011;475(7355):231-234. doi:10.1038/nature10167.
8. Kim TH, Song J, Kim SH, Parikh AK, Mo X, Palanichamy K, et al. Piperlongumine treatment inactivates peroxiredoxin 4, exacerbates endoplasmic reticulum stress, and preferentially kills high-grade glioma cells. *Neuro Oncol* 2014;16(10):1354-1364. doi:10.1093/neuonc/nou088.
9. Zheng J, Son DJ, Gu SM, Woo JR, Ham YW, Lee HP, et al. Piperlongumine inhibits lung tumor growth via inhibition of nuclear factor kappa B signaling pathway. *Sci Rep* 2016;6:26357. doi:10.1038/srep26357.

For more specific information on claims, visit [www.corning.com/certificates](http://www.corning.com/certificates).

**Warranty/Disclaimer:** Unless otherwise specified, all products are for research use only. Not intended for use in diagnostic or therapeutic procedures. Not for use in humans. Corning Life Sciences makes no claims regarding the performance of these products for clinical or diagnostic applications.

For additional product or technical information, visit [www.corning.com/lifesciences](http://www.corning.com/lifesciences) or call 800.492.1110. Outside the United States, call +1.978.442.2200 or contact your local Corning sales office.

# CORNING

**Corning Incorporated**  
*Life Sciences*

836 North St.  
Building 300, Suite 3401  
Tewksbury, MA 01876  
t 800.492.1110  
t 978.442.2200  
f 978.442.2476

[www.corning.com/lifesciences](http://www.corning.com/lifesciences)

**ASIA/PACIFIC**  
**Australia/New Zealand**  
t 61 427286832  
**Chinese Mainland**  
t 86 21 3338 4338  
f 86 21 3338 4300  
**India**  
t 91 124 4604000  
f 91 124 4604099

**Japan**  
t 81 3-3586 1996  
f 81 3-3586 1291  
**Korea**  
t 82 2-796-9500  
f 82 2-796-9300  
**Singapore**  
t 65 6572-9740  
f 65 6735-2913  
**Taiwan**  
t 886 2-2716-0338  
f 886 2-2516-7500

**EUROPE**  
CSEurope@corning.com  
**France**  
t 0800 916 882  
f 0800 918 636  
**Germany**  
t 0800 101 1153  
f 0800 101 2427  
**The Netherlands**  
t 020 655 79 28  
f 020 659 76 73  
**United Kingdom**  
t 0800 376 8660  
f 0800 279 1117

**All Other European Countries**  
t +31 (0) 206 59 60 51  
f +31 (0) 206 59 76 73  
**LATIN AMERICA**  
grupoLA@corning.com  
**Brazil**  
t 55 (11) 3089-7400  
**Mexico**  
t (52-81) 8158-8400